Engineering 6 (2020) 1403–1407

Contents lists available at ScienceDirect

Engineering

journal homepage: www.elsevier.com/locate/eng

Research
Clean Power Technology—Article

Moisture Absorption and Desorption in an Ionomer-Based Encapsulant: A Type of Self-Breathing Encapsulant for CIGS Thin-Film PV Modules

Miao Yang *, Raymund Schäffler, Tobias Repmann, Kay Orgassa

NICE Solar Energy GmbH, Schwaebisch Hall 74523, Germany

ARTICLE INFO

Article history:
Received 2 September 2019
Revised 16 January 2020
Accepted 27 February 2020
Available online 30 October 2020

Keywords:
Ionomer
Encapsulant
Moisture absorption and desorption
Cu(In,Ga)Se_2 photovoltaic module

ABSTRACT

As an alternative to conventional encapsulation concepts for a double glass photovoltaic (PV) module, we introduce an innovative ionomer-based multi-layer encapsulant, by which the application of additional edge sealing to prevent moisture penetration is not required. The spontaneous moisture absorption and desorption of this encapsulant and its raw materials, poly(ethylene-*co*-acrylic acid) and an ionomer, are analyzed under different climatic conditions in this work. The relative air humidity is thermodynamically the driving force for these inverse processes and determines the corresponding equilibrium moisture content (EMC). Higher air humidity results in a larger EMC. The homogenization of the absorbed water molecules is a diffusion-controlled process, in which temperature plays a dominant role. Nevertheless, the diffusion coefficient at a higher temperature is still relatively low. Hence, under normal climatic conditions for the application of PV modules, we believe that the investigated ionomer-based encapsulant can "breathe" the humidity: During the day, when there is higher relative humidity, it "inhales" (absorbs) moisture and restrains it within the outer edge of the module; then at night, when there is a lower relative humidity, it "exhales" (desorbs) the moisture. In this way, the encapsulant protects the cell from moisture ingress.

1. Introduction

Encapsulants, which are chemically stable, compatible with cells, and exhibit high resistance against atmospheric gases, pollutants, radiation, mechanical stress, and so forth, are of great interest for photovoltaic (PV) module manufacturing, especially in terms of reliability [1–5]. Polymer film based on ethylene–vinyl acetate copolymer (EVA) has hitherto been the most widely used encapsulant in single-glass/backsheet c-Si modules [6]. However, many results from research and applications indicate that EVA's potential to release acetic acid under exposure to atmospheric water and/or ultraviolet radiation, along with related problems in reliability, restrict its application, especially for double-glass applications [7,8]. For building-integrated photovoltaic (BIPV) applications, the requirements for the mechanical stability and safety of PV modules are more essential. As a well-known thermoplastic interlayer for laminated safety glass, polyvinyl butyral (PVB), which has higher resistance against mechanical load, has been successfully implemented in BIPVs [9]. The most critical disadvantage of PVB is its high sensitivity to hydrolysis, followed by a high water uptake, which results in a significant decrease of its adhesion to glass [10] and the formation of haze [11]. In recent years, there has been increasing demand for an advanced encapsulation solution based on polyolefin elastomers (POE) arising from PV module manufactures [12]—especially for double-glass c-Si modules and thin-film modules. Unfortunately, the water vapor transmission rate (WVTR) of POE, which is about a few grams per square meter per day according to technical data sheets, is not low enough. The edges of PV modules encapsulated with any of the abovementioned materials must therefore be additionally well sealed against moisture ingress [13,14]. Through our elaborate investigations and perennial application experiences, we report an ionomer-based self-breathing encapsulant film with no edge sealing for our Cu(In,Ga)Se_2 (CIGS) thin-film PV modules.

2. Material and methods

The investigated encapsulation film, which has a multilayer structure consisting of poly(ethylene-*co*-acrylic acid) (EAA) and thermoplastic ionomer (metal-ion-neutralized EAA), is a commercial product provided by our partner company. It has a thickness of

* Corresponding author.
E-mail address: MYang@nice-solarenergy.com (M. Yang).

https://doi.org/10.1016/j.eng.2020.02.020

0.7 mm, an EAA/ionomer volume ratio of 1:2, and a melting point of 98 °C.

In order to investigate their moisture absorption, the encapsulant samples and their corresponding raw material pellet samples were respectively placed in glass bottles and dried in a vacuum dryer (Goldbrunn 450, GOLDBRUNN, Germany) under about 2 kPa at 80 °C for one week. Although a certain amount of residual water should still exist, we define the samples after this treatment as dry samples in this paper. Subsequently, the samples were respectively stored in a climate chamber (VCL 4010, Vötsch Industrietechnik GmbH, Germany) for moisture absorption. Under every set of temperature and relative air humidity (details provided in Section 3.1), one encapsulant sample (~2 g), one EAA pellet sample (~10 g), and one ionomer pellet sample (~10 g) were kept in the chamber until their equilibrium moisture contents (EMCs) were achieved. In order to observe the moisture desorption, samples with saturated moisture contents were stored in a climate housing, where the temperature was kept at 22 °C and the relative air humidity was maintained between 8% and 10%, until a new EMC was reached.

Moisture absorption and desorption in the ionomer encapsulant samples were monitored by an analytical scale (ABT120-5DM, KERN GmbH, Germany). During moisture absorption under given conditions in the climate chamber, the samples were taken out of the chamber after a certain time interval and weighed using a scale as quickly as possible. After that, the samples were placed back into the climate chamber for further absorption. During moisture desorption, the encapsulant samples were weighed *in situ* in the climate housing. The moisture content M is therefore a function of the storage duration t and is proportional to the increase in sample weight $\Delta W(t)$:

$$M(t) = \frac{\Delta W(t)}{W(0)} = \frac{W(t) - W(0)}{W(0)} \quad (1)$$

where $W(0)$ and $W(t)$ represent the weight of the dry sample and its value at t, respectively.

3. Results and discussion

3.1. Moisture absorption

Fig. 1 illustrates the time-dependent moisture absorptions of the ionomer-based encapsulant samples and their pellet raw materials under three climatic conditions: 30 °C and 70% relative humidity (RH; corresponding to an absolute humidity of 21.2 g·m^{-3}); 50 °C and 26% RH (21.5 g·m^{-3}); and 50 °C and 70% RH (57.9 g·m^{-3}). These can be well described using a simplified solution of the second Fick equation [15] with the following form:

$$M(t)/M_\infty = 1 - \exp\left[-7.3(K \cdot t)^{0.75}\right] \quad (2)$$

where M_∞ is the EMC and K is a constant that contains the diffusion coefficient and a geometric factor.

Since the scale of the encapsulant film thickness h is much smaller than its area, we may consider the film as an infinitely large plate; thus, the moisture only diffuses perpendicularly through the film surface into the film. The constant K is therefore a quotient of the diffusion coefficient D against $4h^2$ [15]. Due to the multilayer structure, we further developed Eq. (2) for our case as follows:

$$\begin{aligned} M(t) &= x_{EAA}M_{EAA}(t) + x_{ionomer}M_{ionomer}(t) \\ &= x_{EAA}M_{EAA,\infty}\left\{1 - \exp\left[-7.3\left(D_{EAA}t/\left(4h^2\right)\right)^{0.75}\right]\right\} \\ &\quad + x_{ionomer}M_{ionomer,\infty}\left\{1 - \exp\left[-7.3\left(D_{ionomer}t/\left(4h^2\right)\right)^{0.75}\right]\right\} \end{aligned} \quad (3)$$

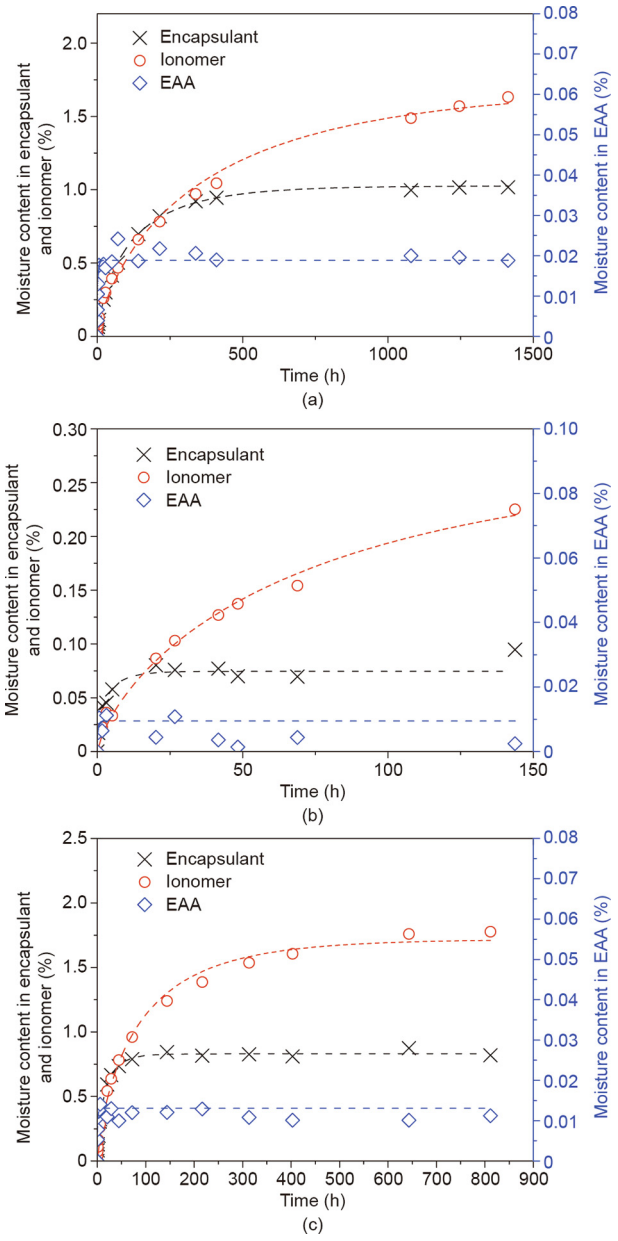

Fig. 1. Moisture absorption by EAA pellets, ionomer pellets, and ionomer-based encapsulant at (a) 30 °C and 70% RH (21.2 g·m^{-3}); (b) 50 °C and 26% RH (21.5 g·m^{-3}); and (c) 50 °C and 70% RH (57.9 g·m^{-3}). The blue and red dashed lines are fitting curves according to Eq. (2), and the black dashed line is a curve-fit according to Eq. (3).

where x_{EAA} and $x_{ionomer} = 1 - x_{EAA}$ represent the content of the EAA and the ionomer, respectively. Using Eqs. (1) and (2), we graphically determined the key parameters to describe the moisture absorption process in both the raw materials and the encapsulant, as listed in Tables 1 and 2, respectively.

The moisture absorption in the investigated encapsulant is due to the fact that the COO^-Me^+ groups in the ionomer are highly polar, with a strong hydrophilic character. Kutsumizu et al. [16] concluded by analyzing sodium-neutralized EAA that each COO^-Na^+ ion pair is able to absorb three water molecules in its vicinity to build a tightly bonded primary hydration shell. As absorption proceeds, the excess water molecules locate around the primary hydration shell. Based on our results, shown in Table 1, we confirm that the polar ionomer is able to absorb more water molecules than the less polar EAA. For the same reason, the

Table 1
EMC M_∞ and constant K of EAA and ionomer pellets, and the adjusted R^2 obtained by fitting the experimental results illustrated in Figs. 1(a)–(c).

Raw material	Climatic conditions	M_∞ (%)	K (min^{-1})	Adjusted R^2
EAA	30 °C, 70% RH (21.2 $g{\cdot}m^{-3}$)	0.019	6.76×10^{-4}	0.98185
	50 °C, 26% RH (21.5 $g{\cdot}m^{-3}$)	0.009	5.00×10^{-3}	0.72203
	50 °C, 70% RH (57.9 $g{\cdot}m^{-3}$)	0.013	1.57×10^{-3}	0.99642
Ionomer	30 °C, 70% RH (21.2 $g{\cdot}m^{-3}$)	1.705	3.09×10^{-6}	0.99266
	50 °C, 26% RH (21.5 $g{\cdot}m^{-3}$)	0.276	1.53×10^{-5}	0.98379
	50 °C, 70% RH (57.9 $g{\cdot}m^{-3}$)	1.720	1.30×10^{-5}	0.99266

Table 2
EMC of each of the components, $M_{EAA,\infty}$ and $M_{ionomer,\infty}$, in the encapsulation film; diffusion coefficient of the water molecules D_{EAA} and $D_{ionomer}$; and the adjusted R^2 obtained by fitting the experimental results illustrated in Figs. 1(a)–(c).

Climatic conditions	$M_{EAA,\infty}$ (%)	$M_{ionomer,\infty}$ (%)	D_{EAA} ($mm^2{\cdot}s^{-1}$)	$D_{ionomer}$ ($mm^2{\cdot}s^{-1}$)	Adjusted R^2
30 °C, 70% RH (21.2 $g{\cdot}m^{-3}$)	0.026	1.550	9.46×10^{-4}	7.74×10^{-7}	0.99858
50 °C, 26% RH (21.5 $g{\cdot}m^{-3}$)	0.025	0.101	1.37×10^{-3}	2.81×10^{-5}	0.97256
50 °C, 70% RH (57.9 $g{\cdot}m^{-3}$)	0.024	1.251	2.15×10^{-4}	6.10×10^{-6}	0.99795

mobility of the water molecules trapped by the COO^-Me^+ ion pair in the ionomer is significantly suppressed, resulting in a much smaller diffusion coefficient (corresponding to a lower WVTR). In 2010, Kempe et al. [14] experimentally characterized the moisture permeation in laminated glasses with different encapsulants. Considering the moisture permeation as a one-dimensional diffusion-controlled process, they determined the diffusion coefficient of water in their investigated ionomer at 85 °C and 85% RH to be 1.25×10^{-4} $mm^2{\cdot}s^{-1}$ (this result is calculated according to the data in Ref. [14]), which is more than one magnitude smaller than the values in EVA (4.01×10^{-3} $mm^2{\cdot}s^{-1}$) and PVB ($1.74 \times 10^{-3} mm^2{\cdot}s^{-1}$), and is in reasonable agreement with our results in Table 2.

At thermodynamic equilibrium, the partial Gibbs energy of a water molecule absorbed in the ionomer encapsulant is identical to that of a free water molecule in the surrounding air, namely $RT\ln(a_w) = RT\ln(p_w/p_{0,w})$, where R and T represents gas constant and temperature, respectively. The thermodynamic activity of absorbed water a_w, which is given by the ratio of the vapor pressure of the water in the encapsulant to the vapor pressure of pure water, is therefore equivalent to the relative air humidity, which corresponds to the ratio of the vapor pressure of the water in air p_w to its saturation vapor pressure $p_{0,w}$. An increase or decrease in air humidity will shift the thermodynamic equilibrium and result in further moisture absorption or desorption, respectively, until a new equilibrium is established.

The establishment of thermodynamic equilibrium is preceded by the homogenization of the absorbed water molecules in the material, which is a diffusion-controlled process. Under constant relative humidity, a higher temperature increases the diffusion coefficient of the water molecules, causing the absorption or desorption to reach its equilibrium faster (results shown in Figs. 1(a)–(c)).

3.2. Moisture desorption

As mentioned above, an encapsulant with saturated moisture content can release the absorbed water molecules if the air humidity of its surroundings decreases. This phenomenon is clearly indicated by the results shown in Fig. 2. As can be seen, although the EMC in the samples is initially unequal, the temporal developments of the moisture content are similar. This means that the kinetics of moisture desorption, and therefore the rate constant of desorption k_{des}, are independent of the amount of adsorbed water molecules. Hence, we describe this kind of water desorption by using the Kissinger analysis for the first-order homogeneous reaction [17] with the following form:

$$\text{Water desorption} = \{1 - K[1 - \exp(k_{des} \cdot t')]\} \times 100\% \quad (4)$$

where $K \propto \exp[-E_{des}/(kT)]$ represents a thermodynamic term and contains an activation energy for desorption E_{des} and Boltzmann constant k; and t' is the water desorption duration. Through mathematic fitting of the curves in Fig. 2, we determine that the water desorption rate constant of the investigated encapsulant samples is equal to 0.02304 h^{-1}.

3.3. Absorption isotherm

Fig. 3 schematically describes the influence of RH on the moisture content at equilibrium M_∞ in the ionomer pellet samples according to our current experimental results. The red dashed line

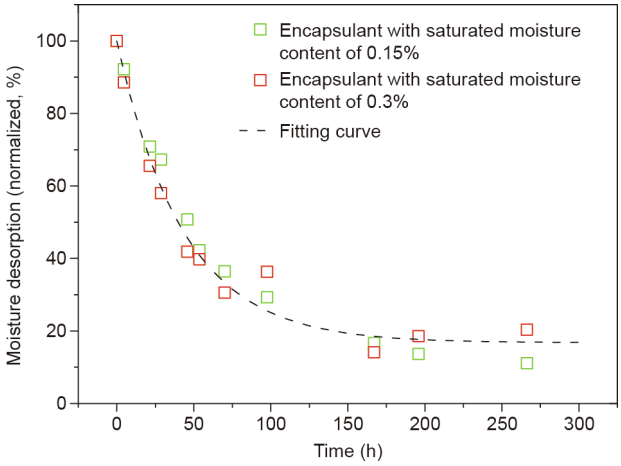

Fig. 2. Moisture desorption of the ionomer-based encapsulant, whose moisture content was saturated at room temperature under two different air humidities. Moisture desorption was realized by storing these samples at room temperature with significantly lower air humidity. The normalized moisture contents, according to the saturated value, are plotted against the storage duration and fitted with a black dashed curve using Eq. (4).

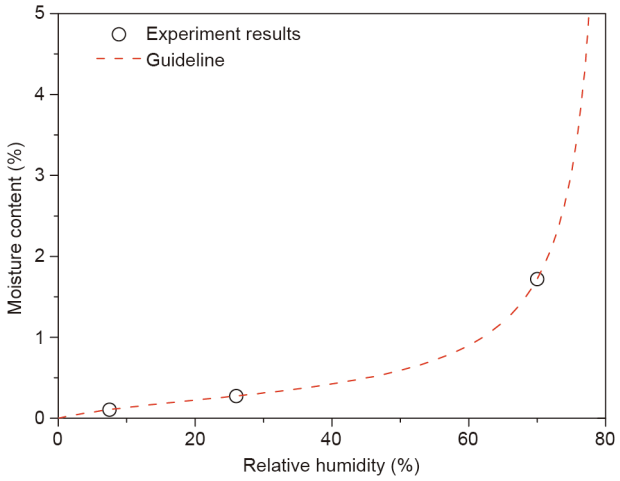

Fig. 3. Sorption isotherm of water molecules for ionomer pellets at 50 °C. The results at 26% RH and 70% RH are graphically determined and listed in Table 1. The result at 7.5% RH was calculated through our previous work (not published). Results are fitted with a red dashed curve using Eq. (5).

is a guideline for the eye, based on the Hailwood–Horrobin equation [18]:

$$RH/M_{\infty} = A + C \cdot RH + B \cdot RH^2 \quad (5)$$

A, *B*, and *C* represent the temperature-related constants, respectively.

Although a more accurate fitting is lacking, the red dashed line in Fig. 3, with A = 0.5278, B = 2.6516, and C = 4.0345, indicates a significant increase of EMC in the ionomer if the relative air humidity is greater than 60%. The line further serves as a guideline for the manufacture of both the encapsulant and the module, in order to control air humidity during production.

3.4. Self-breathing encapsulant

In regard to the spontaneous moisture absorption and desorption, as discussed above, it is reasonable to consider the investigated ionomer-based encapsulant as a self-breathing material that depends on air humidity: During the daytime, when there is comparative higher relative air humidity, the encapsulant absorbs moisture. Thanks to the low diffusion coefficient, as listed in Table 2, most of the absorbed water molecules are concentrated on the very outer edge of the PV module. During the night, the lower air humidity reverses the direction of the thermodynamic process; thus, the encapsulant releases moisture. Therefore, as long as the edge area is wide enough (which is also essential for insulation distance), moisture can scarcely reach the cells under conventional application conditions, and no edge sealing is required.

Compared with other conventional moisture-absorbing encapsulants such as EVA and PVB, we emphasize that the self-breathing function of the ionomer-based encapsulant exhibits two practical and essential advantages: ① No hydrolysis reaction exists, and moisture absorption and desorption in the ionomer-based encapsutant are completely reversible; and ② the diffusion coefficient of water in the ionomer is significantly lower than that in EVA and PVB, as discussed in Section 3.1. Although water diffusion in EAA is comparatively faster, the EMC of EAA, which is about 0.02%, is negligible. Hence, as the presented encapsulant is a combination of these two components, the water penetration depth in it will be much smaller than that in EVA and PVB under the same conditions. According to the results in Ref. [14], 10 h is roughly sufficient for water molecules to penetrate a distance of 10 mm in EVA and PVB at 85 °C and 85% RH. As certificated by TÜV Rheinland, we report that, after a standard 1000 h of damp heat treatment, the power degradation of our CIGS modules, which have an edge width of 8.4 mm and use the ionomer-based encapsulant, is less than 5%, which fulfills the regulation of the international electrotechnical commission standards (IEC 61730).

4. Conclusions

In the present work, we have introduced a promising ionomer-based encapsulant, which is able to spontaneously absorb and/or desorb moisture. This process is thermodynamically driven by the RH of the environment. Furthermore, since the temperature-depended diffusion coefficient of water molecules is relatively low due to the polar nature of the $COO^{-}Me^{+}$ groups in the ionomer, the encapsulant is able to "inhale" moisture when the air humidity is high, and "exhale" it when the air humidity decreases, without letting the moisture ingress into the cells.

Acknowledgements

The support from our partner company in providing the ionomer-based encapsulant samples and the corresponding raw materials as well as the permission for material analysis is fruitfully acknowledged. Special thanks are due to Dr. Gernot Oreski from Polymer Competence Center Leoben GmbH (Austra) for the helpful discussions.

Compliance with ethics guidelines

Miao Yang, Raymund Schäffler, Tobias Repmann, and Kay Orgassa declare that they have no conflict of interest or financial conflicts to disclose.

References

[1] Kempe M. Evaluation of encapsulant materials for PV applications. Photovoltaics Int 2010;9:170–6.
[2] Hasan O, Arif AFM. Performance and life prediction model for photovoltaic modules: effect of encapsulant constitutive behavior. Sol Energy Mater Sol Cells 2014;122:75–87.
[3] Reid CG, Bokria JG, Woods JT. UV aging and outdoor exposure correlation for EVA PV encapsulants. In: Proceedings of the SPIE Reliability of Photovoltaic Cells, Modules, Components, and Systems VI; 2013 Aug 25; San Diego, CA, USA; 2013.
[4] Skoczek A, Sample T, Dunlop ED. The results of performance measurements of field-aged crystalline silicone PV modules. Prog Photovoltaic Res Appl 2009;17 (4):227–40.
[5] Schulze SH, Pander M, Dietrich S, Ebert M. Encapsulation polymers—a key issue in module reliability. Photovoltaics Int 2011;11:156–62.
[6] Omazic A, Oreski G, Halwachs M, Eder GC, Hirschl C, Neumaier L, et al. Relation between degradation of polymeric components in crystalline silicon PV module and climatic conditions: a literature review. Sol Energy Mater Sol Cells 2019;192:123–33.
[7] Czanderna AW, Pern FJ. Encapsulation of PV modules using ethylene vinyl acetate copolymer as a pottant: a critical review. Sol Energy Mater Sol Cells 1996;43:101–81.
[8] De Oliveira MCC, Diniz ASAC, Viana MM, de Freitas VCL. The causes and effects of degradation of encapsulant ethylene vinyl acetate copolymer (EVA) in crystalline silicon photovoltaic modules: a review. Renew Sustain Energy Rev 2018;81(2):2299–317.
[9] Wang Y, Hassanien R, Li M, Xu G, Ji X. An expermental study of building thermal environment in building integrated photovoltaic (BIPV) installation. Bulg Chem Commun 2016;48E:158–64.
[10] Tupý M, MěřínskáD SP, Kalendova A, Klásek A, Zvoníček J. Effect of water and acid–base reactants on adhesive properties of various plasticized poly(vinyl butyral) sheets. J Appl Polym Sci 2012;127(5):3474–84.
[11] Park H, Jeong J, Shin E, Kim S, Yi J. A reliability study of silicon heterojunction photovoltaic modules exposed to damp heat testing. Microelectron Eng 2019;216:111081.
[12] Govaerts J, Geyer B, van der Heide A, Borgers T, Hellström S, Broeders B, et al. Extended qualification testing of 1-cell crystalline Si PV laminates: impacts of advanced cell metallization and encapsulation schemes. In: Proceeding of the

33rd European Photovoltaic Solar Energy Conference and Exhibition; 2017 Sep 25–29; Amsterdam, Holland; 2017.
[13] Westin PO, Neretnieks P, Edoff M. Damp heat degradation of CIGS-based PV modules. In: Proceeding of the 21st European Photovoltaic Solar Energy Conference; 2006 Sep 4–8; Dresden, Germany; 2006.
[14] Kempe M, Dameron A, Moricone T, Reese M. Evaluation and modeling of edge-seal materials for photovoltaic applications. In: Proceeding of the 35th IEEE Photovoltaic Specialists Conference; 2010 Jun 20–25; Honolulu, HI, USA; 2010.
[15] Chen CH, Springer G. Moisture absorption and desorption of composite materials. J Compos Mater 1976;10(1):2–20.
[16] Kutsumizu S, Nagao N, Tadano K, Tachino H, Hirasawa E, Yano S. Effects of water sorption on the structure and properties of ethylene ionomers. Macromolecules 1992;25:6829–35.
[17] Kissinger HE. Reaction kinetics in differential thermal analysis. Anal Chem 1957;29(11):1702–6.
[18] Hailwood AJ, Horrobin S. Absorption of water by polymers: analysis in terms of a simple model. S Trans Faraday Soc 1946;42B:84–92.